KSME International Journal, Vol. 17 No. 1, pp. 157~167, 2003

Quantitative Vapor Phase Exciplex Fluorescence Measurements at High Ambient Temperature and Pressure

Tongwoo Kim*, Jaal B. Ghandhi

Engine Research Center, University of Wisconsin-Madison, 1500 Engineering Drive, Madison, Wisconsin 53706, USA

The exciplex fluorescence technique with the TMPD (tetamethyl-*p*-phenylene-diamine)/naphthalene dopant system was applied in a combustion-type constant-volume spray chamber. A detailed set of calibration experiments has been performed in order to quantify the TMPD fluorescence signal. It has been demonstrated that the TMPD fluorescence intensity was directly proportional to concentration, was independent of the chamber pressure, and was not sensitive to quenching by either water vapor or carbon dioxide. Using a dual heated-jet experiment, the temperature dependence of TMPD fluorescence up to 1000 K was measured. The temperature field in the spray images was determined using a simple mixing model, and an iterative solution method was used to determine the concentration and temperature field including the additional effects of the laser sheet extinction. The integrated fuel vapor concentration compared favorably with the measured amount of injected fuel when all of the liquid fuel had evaporated.

Key Words : Exciplex Fluorescence Technique, Calibration of the TMPD Fluorescence, Photo-Physical Effect on Thermodynamic Condition, Spatial Distribution of Equivalence Ratio and Temperature

Nomenclature

c_p : Specific heat
C_{gas} : TMPD concentration [mol/ℓ]
f : Photophysical function defined as Eq. (3)
hc/λ : Energy of the fluorescence photon
h_v : latent heat of vaporization
I_0 : Incident intensity of the laser sheet [W/cm^2]
K : Absolute calibration constant
L : Distance that the laser sheet has traveled [cm]
MW : Molecular weight
N : Number density [cm^{-3}]
P : Pressure
R : Gas constant
S : Spray tip penetration or pixel intensity on the camera [pixel count]
T : Temperature
t : Time
V : Measurement volume
x : Spray axial position or mole fraction
y : Spray radial position

Greek symbols

ε : Molar extinction coefficient [(ℓ/mol-cm]
Φ : Local equivalence ratio within the fuel vapor field
ϕ : Fluorescence efficiency (Stern-Vollmer factor)
η_c : Detection effincy
λ : Wavelength
θ : Spray spreading angle
ρ : Ratio of the fuel to the ambient density
σ : Absorption coefficient [cm^2] or unit standard deviation

* **E-mail** : tongwoo@cae.wisc.edu
TEL : +1-608-263-1598; **FAX** : +1-608-263-9870
Engine Research Center, University of Wisconsin-Madison, 1500 Engineering Drive, Madison, Wisconsin 53706, USA. (Manuscript **Received** July 4, 2002; **Revised** October 22, 2002)

Ω : Collection solid angle

Subscripts

a or amb : Ambient
cal : Calibration reference condition
f : Fuel
i : Initial state
int : Intermediate state at which the fuel vaporized
LIF : laser induced fluorescence
l or $liquid$: liquid
mix : Adiabatic (final) mixture state
st : Stoichiometric condition
v or $vapor$: Vapor

1. Introduction

Several techniques have been developed to quantitatively measure the vapor fuel concentration in evaporating sprays (Zhao and Ladommatos, 1998). Raman spectroscopy (Scheid et al., 1986 ; Rabenstein et al., 1998) has been used for single-point measurement of local fuel-air ratio in a diesel jet in a constant volume chamber. Raman scattering can be highly quantitative, but single-point measurements require a long time to completely characterize the spatial and temporal spray distribution. To overcome this limitation, planar laser-based imaging diagnostics using Rayleigh scattering (Espey et al., 1997), Mie scattering (Kosaka and Kamimoto, 1993 ; Bruneaux, 2001) and exciplex laser-induced fluorescence (LIF) (Felton et al., 1993 ; Yeh et al., 1994 ; Kim and Ghandhi, 2001) have been applied to evaporating fuel sprays. The Rayleigh scattering technique has the advantage that no tracer needs to be added to the fuel. However, Rayleigh scattering cannot be used to investigate the whole spray structure due to elastic scattering from droplets. The Mie scattering technique utilizes a low volatility oil added to the fuel as a marker for the vapor-phase fuel. This technique has limitations due to the Mie scattering dependence on drop size, and has a limited temperature range, which is constrained by the boiling point of the additive oil.

The exciplex (excited state complex) laser-induced fluorescence (LIF) technique relies on a spectral shift between liquid- and vapor-phase fluorescence to allow simultaneous visualization of both phases in an evaporating fuel spray (Melton, 1983). Two fluorescent dopants are added to the fuel ; for diesel fuel experiments TMPD (tetramethyl-*p*-phenylene-diamine) and naphthalene are the most common dopants. The monomer, TMPD, absorbs the laser light, and directly fluoresces in the vapor phase. In the liquid phase the excited monomer preferentially reacts with the second dopant, naphthalene, to form an excited complex, the exciplex. The fluorescence from the exciplex is red-shifted from the monomer fluorescence by an amount equivalent to the binding energy difference. The difficulties that arise with this method are the temperature dependence of the monomer fluorescence, fluorescence quenching by oxygen, cross-talk between the monomer (vapor) and exciplex (liquid) fluorescence due to an overlap of the emission spectra, and quantification of the liquid signal.

Several studies have applied the exciplex technique to diesel sprays. Rotunno et al. (1990) presented a direct calibration procedure for the vapor phase concentration in the range from 313 K to 443 K, and quantitatively showed the transient behavior of the vapor and liquid phases in an evaporating spray. Felton et al. (1993) applied the technique to a hollow-cone spray in a two-stroke engine. They showed that the absorption of the TMPD dopant increased sharply as the temperature exceeded 500 K. Therefore, quantitative measurement of vapor phase fuel concentration at temperatures above 500 K would require measurement of the local gas temperature. Yeh et al. (1994) reported quantitative fuel vapor concentration in a rapid compression machine. They found that thermal decomposition of TMPD during the injection and the vaporization time, ~10 ms, was negligible at 20 bar and 750 K. The TMPD fluorescence intensity was calibrated in a range from 500 to 800 K, and they showed that the absorbance of TMPD vapor was minimally affected by temperature, contrary to the result by Felton. Senda and Kanda (1997) applied the exciplex method to an impinging spray

with a temperature of 700 K and a pressure of 25 bar. The vapor concentration was assessed quantitatively by applying Lambert-Beer's law to the measured fluorescence intensity, and by considering the quenching process of the fluorescence emission by the fuel concentration as well as temperature in a range from 550 K to 700 K.

The objective of this paper is to present a complete calibration of the TMPD fluorescence signal over the range of conditions expected for DI diesel operation. The exciplex LIF technique was applied to quantitatively measure the fuel vapor concentration in a combustion-type spray chamber. The total vapor mass in these measurements was found to agree very well with the known mass of fuel injected.

2. Experimental Apparatus

2.1 Constant-volume combustion-type spray chamber

A constant-volume combustion-type spray chamber was used in this work. The chamber allows spark ignition and combustion of a homogeneous mixture of acetylene, oxygen, and nitrogen at the desired chamber density. Following the premixed combustion, the high temperature products cool down due to heat transfer to the chamber walls. At the appropriate time (desired bulk temperature) the fuel is injected into the chamber. The use of premixed combustion and the subsequent cooling process in the constant volume chamber to match a state representative of conditions in a diesel engine at the start of fuel injection is similar to that of Oren et al. (1984), and Naber and Siebers (1996).

Figure 1 shows a cross section of the spray chamber. The chamber was disk-shaped, with a 10 cm diameter and 5 cm depth. The chamber mixture was prepared by first evacuating the chamber, then filling the mixture sequentially with acetylene (4.7%), air (53%) and then nitrogen (42%). The gases were well mixed by the momentum of the incoming mixtures. The reactant molar composition was 4.7% acetylene, 11% oxygen and 84% nitrogen, and the combustion product composition was 85% nitrogen, 4.7% H_2O and 9.4% CO_2. The chamber density was limited to 15 kg/m^3 by the large quartz window.

Figure 2 shows average pressure traces acquired at a chamber density of 15 kg/m^3 both without fuel injection (dashed) and with fuel injection occurring 1 s after ignition (solid) corresponding to a temperature of 1200 K. The difference between the two traces following the injection time is the result of the latent heat of vaporization of the liquid fuel. Also shown in Fig. 2 at a time of 400 ms after spark ignition is the 95% confidence interval for the chamber pressure, and shows that excellent run-to-run

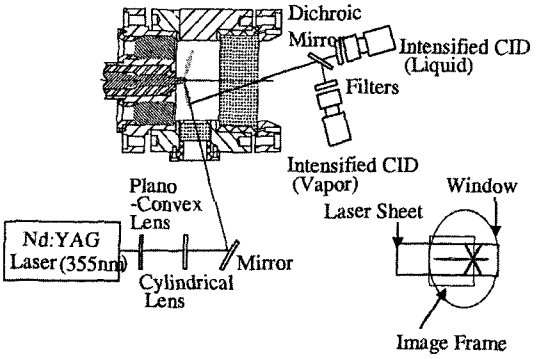

Fig. 1 Schematic of constant volume chamber and optical imaging system, and view of camera when aligned normal to spray axis

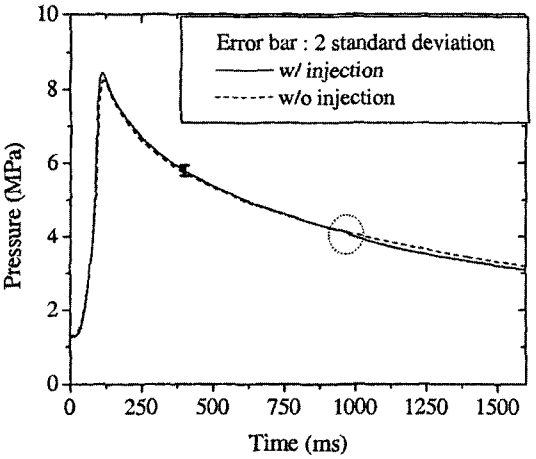

Fig. 2 Pressure history of the combustion-type spray chamber for an ambient density of 15 kg/m^3. The circled area shows the effect of fuel vaporization (injection) on the chamber pressure

repeatability was achieved for the premixed combustion.

The chamber gas temperature was measured using a compensated thermocouple and found to be nearly homogeneous spatially at injection times corresponding to a temperature of 1000 K. Run-to-run variations of 50 K were observed in the single-point temperature data due to the effect of turbulence, but the bulk gas temperature is expected to be more repeatable than the measured instantaneous local value based on the high degree of repeatability of the chamber pressure from run to run. In addition, the effect of water condensation on the chamber density at the time of injection was found to be negligible. For the further details of the facility see references (Kim and Ghandhi, 2001 ; Kim, 2001).

2.2 High pressure injection system

An hydraulic-actuated electronically controlled unit injector (Caterpillar HEUI 90) was investigated. The production oil manifold was used to retain the dynamic characteristics, but the solenoid was driven by an external high voltage injector driver to allow single shot operation. Details of the injector can be found in Table 1. The injection pressure was 90 MPa, and the nozzle hole size was 158 μm.

Table 1 Injector system specifications and the conditions tested

Caterpillar HEUI 90 injector	
Nozzle type	VCO nozzle
Number of nozzle	6 holes
Nozzle diameter	158 μm
Spray angle	145 degree
Injection duration	1.4 ms
Peak inj. pressure	90 MPa
Injected fuel amount	4.5 mg/hole
Fuel line temperature	298 K

Table 2 Exciplex dopant system

Doped fuel	% weight	Boiling pt. (K)/1atm	Mol. wt. (g/mol)
n-dodecane ($C_{12}H_{26}$)	90	489	170
Naphthalene ($C_{10}H_8$)	9	491	128
TMPD ($C_{10}H_{16}N_2$)	1	533	164

The exciplex-forming dopants used are shown in Table 2. To limit the amount of doped fuel required, a small volume fuel delivery system was used. The system consisted of a pressurized reservoir connected to the injector via a 7 μm filter. Nitrogen was used to pressurize the doped fuel to the same pressure, 3 bar, as the original fuel pump system. A comparison of spray penetration data showed no discernable difference between the modified fuel system and solenoid driver and the original injector driver and fuel pump system (Kim, 2001).

2.3 Exciplex LIF optical system

Figure 1 shows the schematic of the optical system used in this experiment. The frequency-tripled output of a Nd : YAG laser (355 nm, 13.5 mJ per pulse and 10 ns pulse width) was formed into a sheet using a 150 mm focal length cylindrical lens and a 1 m focal length plano-convex lens. The thickness of the laser sheet was approximately 400 μm. The laser sheet was aligned with the axis of a single spray plume, and the imaging system was oriented perpendicular to the laser sheet. For simultaneous detection of both the liquid- and the vapor-phase signals, two intensified 8-bit CID cameras were used in conjunction with a 45 degree angle of incidence dichroic mirror (90% reflectance for $380<\lambda<450$ nm, and 85% transmittance for $\lambda>525$ nm). The intensifier gate width was 100 ns to isolate the fluorescence from luminosity of the premixed combustion. To isolate the liquid-phase exciplex fluorescence signal a long pass ($\lambda>505$ nm) filter was used. To isolate the vapor-phase monomer fluorescence signal a broad band interference filter (centered at 400 nm with a full width at half maximum of 25 nm) and a Schott glass filter (GG385) were used.

3. Vapor Phase Calibration

Based on photophysics, the vapor-phase fluo-

rescence signal, N_{LIF}, at the detector [photon/s] can be written as

$$N_{LIF}=\frac{I_0\cdot\eta_c\cdot\Omega\cdot V}{(hc/\lambda)}\cdot N_{TMPD}\cdot\sigma_{TMPD}/4\pi\cdot\phi_{TMPD} \quad (1)$$

where I_0 is the incident intensity of the laser sheet [W/cm^2], η_c is the detection efficiency composed of filter transmission and the camera fill factor, Ω is the collection solid angle [sr], V is the measurement volume [cm^3], hc/λ is the energy of the fluorescence photon [J], N_{TMPD} is the number density of TMPD molecules [cm^{-3}], $\sigma_{TMPD}/4\pi$ is the differential absorption cross-section of the TMPD fluorescence [cm^2/sr], and ϕ_{TMPD} is the TMPD fluorescence efficiency (Stern-Vollmer factor). By integrating with respect to time and collecting constant terms, this expression for a data image can be written more simply as

$$S_{LIF}=K\cdot N_{TMPD}\cdot\bar{\sigma}_{TMPD}\cdot\bar{\phi}_{TMPD} \quad (2)$$

where S_{LIF} represents the pixel intensity on the camera [pixel count], K is a calibration constant [(pixel count)/cm^{-3}] obtained at a reference condition as described below, and $\bar{\sigma}_{TMPD}$ and $\bar{\phi}_{TMPD}$ are the photophysical parameters normalized by their values at the calibration reference condition. In order to calibrate absolutely, the constant K must be determined, and the dependences of $\bar{\sigma}_{TMPD}$ and $\bar{\phi}_{TMPD}$ on temperature, pressure and collision partner must be fully understood. Each of these parameters has been independently investigated, see Kim and Ghandhi (2001) for details, and only the results are summarized here for brevity.

The absolute calibration was obtained by imaging a heated jet with a known TMPD concentration installed in the spray chamber. Results from the absolute calibration experiment (which was performed at the start of each test run) are shown in Fig. 3. The fluorescence signal is seen to exhibit excellent linearity with variations in the TMPD concentration in Fig. 3. The observed change in the TMPD fluorescence (S_{LIF}) with TMPD number density (N_{TMPD}) directly provided the calibration constant, K, in Eq. (2).

The absorption cross-section and fluorescence efficiency ($\bar{\sigma}_{TMPD}$ and $\bar{\phi}_{TMPD}$) are known to depend on the local thermodynamic conditions (temperature and pressure), and on the local composition through the quenching efficiencies of different species. Figure 4 shows the result of the bulk gas pressure effect on TMPD fluorescence. It can be seen that the bulk gas pressure does not affect the TMPD fluorescence. This result allows all other evaluation of the photophysical parameters to be performed at ambient pressure. Also, the lack of a pressure effect indicates that collisional quenching is not responsible for the fluorescence behavior since the collision frequency ($\propto$ mixture pressure) varies

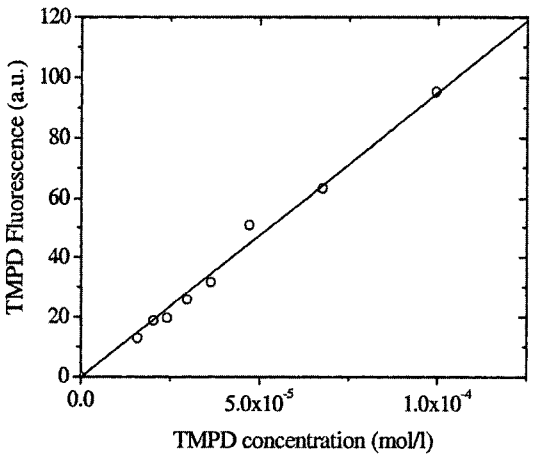

Fig. 3 Calibration relationship between TMPD concentration and fluorescence signal

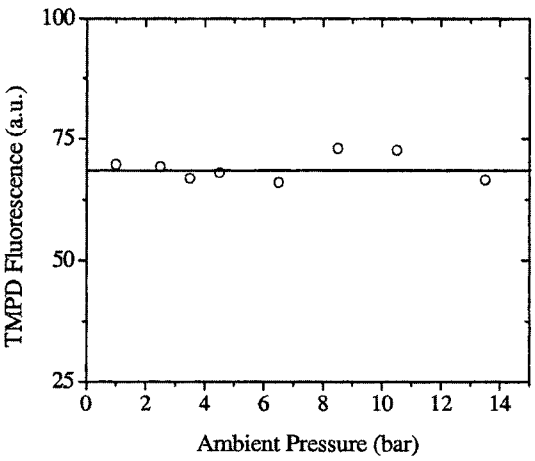

Fig. 4 TMPD fluorescence dependence on ambient pressure

by a factor of 15 in these data with no difference in the fluorescence signal.

Figures 5 and 6 show the result of the effect of collision partner on TMPD fluorescence. The fluorescence of TMPD is not affected by CO_2 (or argon) and water vapor, the major constituents of the combustion products in the chamber at the time of injection. Therefore, it was found that the composition of the combustion products would not affect the calibration of the TMPD vapor signal.

Temperature has been shown to significantly affect the fluorescence (both σ and ϕ) of TMPD

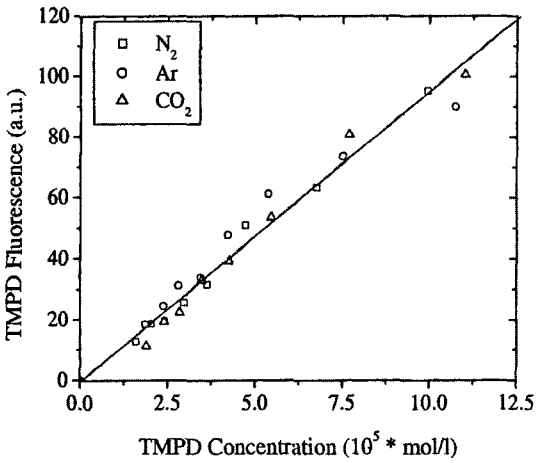

Fig. 5 TMPD fluorescence dependence on collision partner

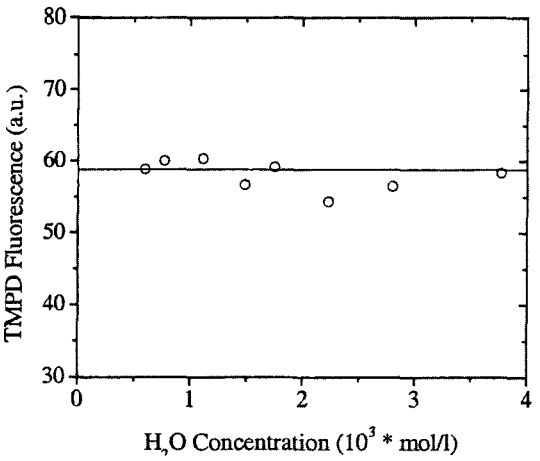

Fig. 6 TMPD fluorescence dependence on water vapor concentration

in all of the previous calibration attempts in the literature. A function, f, that incorporates the temperature dependence of the photophysical parameters can be defined as

$$f(T) \equiv \bar{\sigma}_{TMPD}(T) \cdot \bar{\phi}_{TMPD}(T) = \frac{\sigma(T)}{\sigma(T_{cal})} \cdot \frac{\phi(T)}{\phi(T_{cal})} \quad (3)$$

Using a dual heated jet experiment, where one jet was heated and the other held at the reference condition, the function $f(T)$ was evaluated, and the result is shown in Fig. 7. It can be seen that the effect of temperature is to first increase the fluorescent yield up to 600 K, then decrease the fluorescent yield as the temperature further increases. These data reflect the trends reported in the literature, which up to this point had appeared to be contradictory. Felton et al. (1993) reported an increase in the fluorescence with temperature and related it to an increase in the absorption cross section, but their data were acquired below 600 K. In other studies the TMPD fluorescence was found to decrease with temperature (Yeh et al., 1994 ; Senda and Kanda, 1997), but these data were acquired at temperatures above 600 K. The multi-valued response shown in Fig. 7 suggests that TMPD would not be a good dopant for thermometry, however, the data of Fig. 7 will allow a quantification of the vapor concentration.

The local temperature in the vapor plume was estimated thermodynamically with the assump-

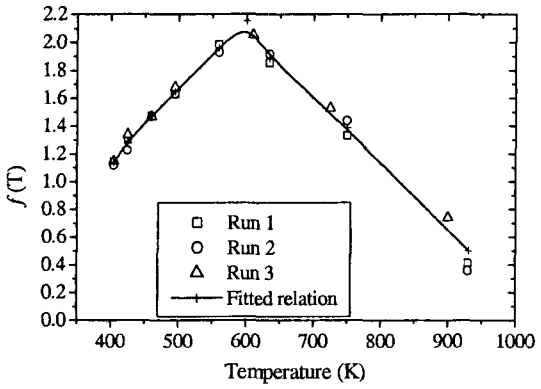

Fig. 7 TMPD fluorescence dependence on temperature

tion of adiabatic mixing between the fuel and air (El-Wakil et al., 1956). Assuming the same saturation temperatures and evaporation rates of the fuel and TMPD, the bulk mean temperature (T_{mix}) in the region where all fuel was vaporized was calculated as follows (El-Wakil et al, 1956);

$$\int_{T_{mix}}^{T_{amb}} c_{p,a}dT = \chi_{F/A}\left[\int_{T_{f,i}}^{T_{int}} c_{p,liquid}dT + h_{v,T_{int}} + \int_{T_{int}}^{T_{mix}} c_{p,vapor}dT\right] \quad (4)$$

where T_{amb} is the temperature of the gas entrained into the spray [K], $c_{p,a}$ is the specific heat of the ambient gas [J/mol-K], $\chi_{F/A}$ is the mole fraction of fuel, $T_{f,i}$ is the initial temperature of the liquid fuel [K], T_{int} is the intermediate temperature at which the fuel vaporizes [K], $h_{v,T_{int}}$ is the latent heat of vaporization at the intermediate temperature [J/mol], and $c_{p,vapor}$ is the specific heat of the fuel vapor [J/mol-K]. Thermodynamic and physical property data of the doped fuel were determined for an assumed mixture of 90% dodecane and 10% naphthalene since data for TMPD were not available (Yaws, 1992 and Vargaftik, 1983). The mixture data were determined using Dalton and Raoult's laws applied to the vapor and liquid phase, respectively. The initial liquid fuel temperature may be higher than the fuel supply temperature, 293 K, due to heat transfer from the premixed combustion to the injector as well as viscous energy dissipation through the injector hole, but the sensitivity of T_{mix} to this was found to be small.

The absorption of the incident beam was calculating using the Lambert-Beer's law as

$$\frac{I(x, y)}{I(0, y)} = 10^{-\int_0^L \varepsilon \cdot C_{gas} dl} = \exp\left[-\int_0^L \sigma_{TMPD} \cdot N_{TMPD}(x, y)\, dl\right] \quad (5)$$

where $I(x, y)$ is the intensity at the pixel of interest, $I(0, y)$ is the incident intensity of the laser sheet before experiencing any extinction, ε is the molar extinction coefficient [l/mol-cm], C_{gas} is the TMPD concentration [mol/l], and L is the distance that the laser sheet has traveled [cm]. The literature value of ε=650 l/mol-cm, (Berman, 1971) was used for this experiment.

The combined effect of temperature and absorption is provided by modifying Eq. (2) to be

$$S_{LIF}(x, y) = K \cdot N_{TMPD}(x, y) \cdot \frac{I(x, y)}{I(0, y)} \cdot f(T(x, y)) \quad (6)$$

The final calculation of TMPD concentration and temperature was obtained by iteratively solving Eqs. (4)-(6) until the change in the fuel concentration fell below a specified threshold.

The local equivalence ratio, Φ, within the fuel vapor field can be calculated based on the local fuel number density and the thermodynamic conditions as

$$\Phi(x, y) = \frac{1-x_{f,st}}{x_{f,st}} \frac{N_f(x, y)}{P\tilde{N}/R \cdot T(x, y) - N_f(x, y)} \quad (7)$$

where $x_{f,st}$, is the stoichiometric mole fraction of fuel (taken as 0.0135 for diesel fuel), N_f is the measured fuel number density [cm^{-3}] obtained from the measured TMPD number density and the doping rate, P is the pressure, $\tilde{N}$ is Avogadro's number, T is the local temperature and R is the gas constant.

A rigorous uncertainty analysis was performed assuming that variation in the independent parameters was uncorrelated. Using Eq. (6) and assuming the uncertainties of the independent variables as their unit standard deviation, then the relative uncertainty in the estimated TMPD number density is

$$\frac{\delta N_{TMPD}}{N_{TMPD}} = \sqrt{\left(\frac{\sigma_K}{K}\right)^2 + \left(\frac{\sigma_{N_{LIF}}}{N_{LIF}}\right)^2 + \left(\frac{\sigma_{I_i}}{I_i}\right)^2 + \left(\frac{\sigma_f}{f}\right)} \quad (8)$$

Therefore, the accuracy of the measurements depends on uncertainties in the absolute calibration (±12.5%), camera noise (±5.0%), pulse-to-pulse laser energy variations (±3.6%), and the quality of the temperature dependence function (±3.9%). As well, the estimations of the temperature field and absorption coefficient may have uncertainties (conservatively ±15.8%). Therefore, the overall estimated uncertainty for the concentration measurement was found to be 21%. Details of the estimation of each uncertainty can be found in Kim (2001).

4. Result and Discussion

The temporal evolution of the spatial dist -ibution of equivalence ratio and temperature that result from the calibration procedure described above for the ambient density and temperature of 15 kg/m^3 and 1000 K, a nozzle hole size of 158 μ m, and an injection pressure of 90 MPa is shown in Fig. 8. As a matter of convenience, the liquid phase extent is shown graphically as an elliptical region superimposed on the image. The injector tip position is shown with a cross and the axes are given as distance from the injector tip in mm. The gray scale shown to the right indicates the temperature or equivalence ratio correspondence, and solid contour lines are shown at increments of 1 in equivalence ratio and −100 K in temperature.

During the earliest stages of the injection, liquid and vapor coexist at the leading edge of the jet. Following this initial phase of the spray penetration the liquid phase penetration actually retracts slightly while the vapor phase continues to penetrate at the leading edge of the jet. This pattern, an intact liquid region that has a finite length and the jet leading edge defined by the vapor phase fuel, persists through the remainder of the injection. Shortly after the end of injection the liquid core detaches from the nozzle, convects downstream and rapidly vaporizes.

The distribution of local temperature, shown in Fig. 8(b), displays the same spatial shape as the equivalence ratio due to the direct (albeit not linear) relationship between the two quantities, see Eq. (4). The temperature depression in the spray is seen to be quite significant; for instance, at 1.0 ms ASI (after the start of injection) it approaches 250 K at the ambient gas temperature of 1000 K.

To verify the liquid-phase exciplex data, a comparison was performed of the liquid-phase exciplex penetration data to penetration data acquired from Mie scattering images at the same conditions. The results are shown in Fig. 9. The Mie scattering data were acquired using a high-speed camera (Kodak model 4540) combined with a high repetition rate diode-pumped Nd: YAG laser (Lee Laser Inc). A 532 nm narrow

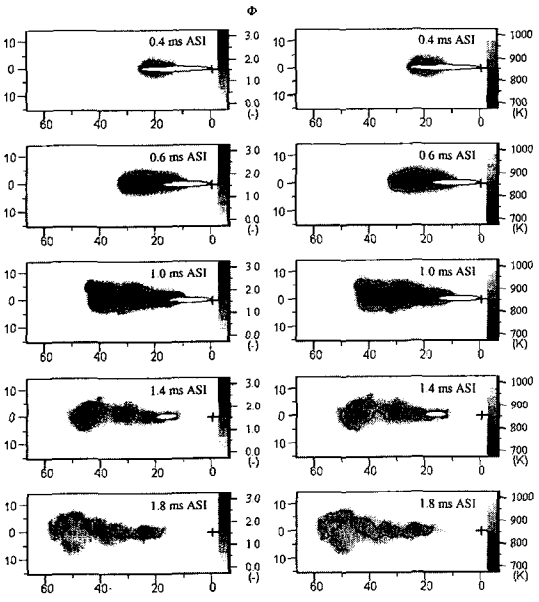

Fig. 8 Quantitative images of equivalence ratio (left) and temperature (right) at the ambient density of 15 kg/m^3 and temperature of 1000 K. The solid lines in the images, shown for convenience, represent the contours with increments of 1 for equivalence ratio and −100 K for temperature from the ambient values (0 and 1000 K), respectively

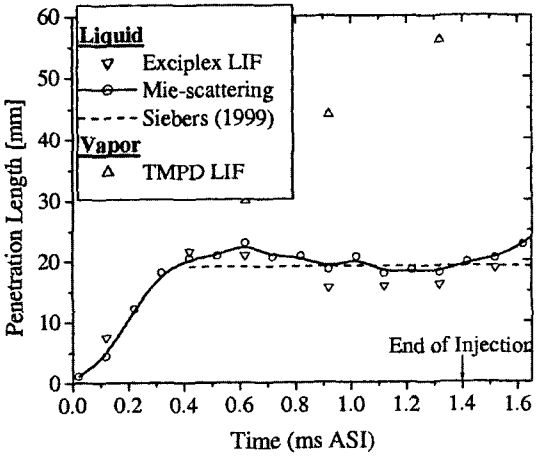

Fig. 9 Comparison of liquid penetration length between Mie scattering signal and the exciplex (liquid) fluorescence signal at the density of 15 kg/m^3, and temperature of 1200 K

band pass filter was used to eliminate any residual flame luminosity. A threshold at 3 times of the background noise was used to define the spray penetration length along the spray axis. As a reference, an estimate of the intact liquid length by the relation of Siebers (1999) is also shown. For this estimation, the area-contraction coefficient used was assumed to be 0.8, and the spray-spreading angle used was obtained from the empirical relationship of Siebers (1999) because of the difficulty in defining the angle from single-shot transient spray images. Figure 9 shows that the intact liquid length measured by both techniques are in good agreement, and match the estimated intact liquid length very well. Therefore, the liquid phase extent is believed to be well represented by the exciplex technique.

To assess the accuracy of the calibration procedure for vapor phase concentration measurement, the 2-D fuel vapor concentration was integrated assuming an axisymmetric vapor distribution and this result was compared with the known mass of fuel injected. Figure 10 shows the histogram of the integrated fuel vapor mass normalized by the known fuel mass (measured gravimetrically) compiled from a total of 18 images corresponding to different experiment dates, different ambient temperature, different injection pressures, and different nozzle hole sizes (Kim, 2001). The mean and standard deviation for 18 data are 0.9 and 0.14 respectively, which may have resulted from the limited dynamic range of the measurement, the lack of axisymmetry of individual images and the observed 10% (maximum) shot-to-shot variations of the injected fuel amount. Given the substantial difference between the calibration condition (P=1 bar, T=430 K) and the experiment conditions (P=35 bar, T=1000 K) this is considered to be good agreement.

The general structure of the evaporating spray observed in these measurements is in excellent agreement with previous researchers. The existence of a finite intact liquid length is consistent with other investigators (Browne, 1986; Espey and Dec, 1995; Naber and Siebers, 1996). The vapor concentration observed in the measurements also agrees with previous studies. Espey et al. (1997) acquired vapor concentration using planar Rayleigh scattering in an engine for a condition where the ambient temperature and density were estimated to be 1050 K and 16.5 kg/m^3. In their images near 0.63 ms after start of injection, the equivalence ratio in the majority of the leading portion of jet ranged from 2 to 4. Their measurements closely compare to these data at a time of 0.6 ms ASI presented in Fig. 8 (an equivalence ratio in the range from 2 to 3) although no attempt was made to match the injection charac-

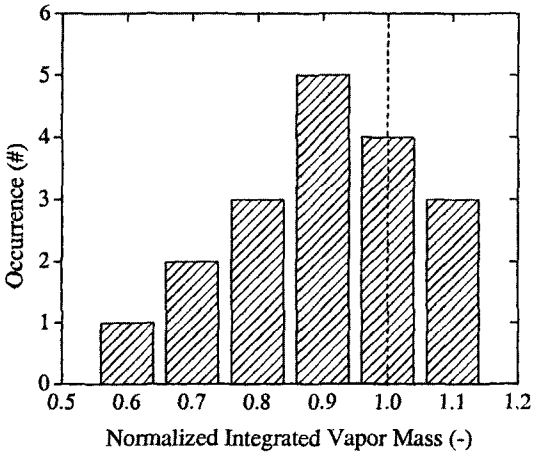

Fig. 10 Integrated fuel vapor mass histogram obtained from a total of 18 images captured at times when all of the fuel had vaporized

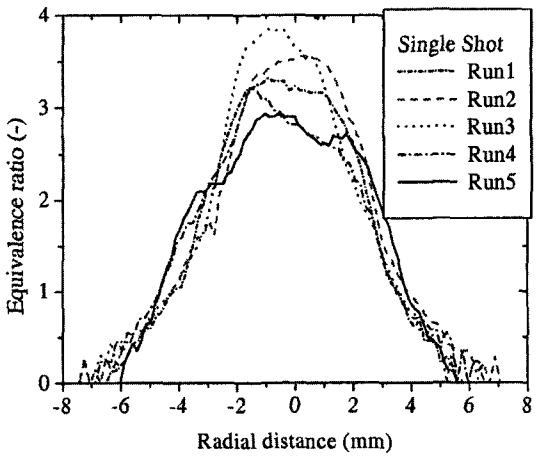

Fig. 11 Radial equivalence ratio profiles across the jet acquired 30 mm downstream from the injector tip

teristics between the two experiments. In addition, Rabenstein et al. (1998) reported values of equivalence ratio of ~3 using Raman scattering for a 90 MPa injection pressure and ambient condition of 20 kg/m^3 and 723 K, also in good agreement with the present results.

Radial equivalence ratio profiles provide information about the mixing of the fuel-vapor and entrained air. Figure 11 shows 5 individual radial equivalence ratio profiles acquired 30 mm downstream from injector tip. The profiles are seen to have wide extent of fuel rich concentration, and the radial profile exhibits a nearly Gaussian shape as compared to the top-hat shape reported by Espey et al. (1997). Bruneaux (2001) and Yeh et al. (1994), however, presented results that agree with the present results. Careful attention to camera focusing was undertaken in present work, and is not the cause for the observed behavior (Kim, 2001).

5. Conclusion

The major results are as follows:

(1) A complete investigation of the issues related to the calibration of the TMPD fluorescence was performed. This included development of a method for the absolute calibration of the imaging system at a reference condition and the application of corrections to this calibration based on the local thermodynamic conditions which affect the photophysical parameters. The effect of pressure and collision partner were found to be negligible, and the effect of temperature was found to increase the fluorescent yield up to 600 K, then decrease it for further increases in temperature. An adiabatic mixing model for the temperature reduction due to vaporization and laser sheet absorption were both accounted for in the final calibration procedure.

(2) The exciplex LIF technique was applied to quantitatively measure the vapor-phase fuel concentration in an evaporating spray under engine-like conditions, a chamber density of 15 kg/m^3 and temperature of 1000 K. The temporal evolution of the spatial distribution of equivalence ratio and temperature were obtained from the calibration procedure. The integrated fuel vapor concentration agreed well with the mass of fuel injected at times when all the liquid fuel was vaporized. The general structure and absolute fuel vapor concentration of the evaporating spray observed in these measurements was in excellent agreement with previous results.

References

Berlman, I. B., 1971, *Handbook of Fluorescence Spectra of Aromatic Molecules*, 2nd edition, Academic Press.

Browne, K., Partridge, I., and Greeves, G., 1986, "Fuel Property Effects on Fuel/Air Mixing in an Experimental Diesel Engine," SAE 860223.

Bruneaux, G., 2001, "Liquid and Vapor Spray Structure in High Pressure Common Rail Diesel Injection," *Atomization and Sprays*, Vol. 11.

El-Wakil, M., Myers P. and Uyehara, O., 1956, "Fuel Vaporization and Ignition Lag in Diesel Combustion," SAE Paper 560063.

Espey, C. and Dec, J., 1995, "The Effect of TDC Temperature and Density on the Liquid -Phase Fuel Penetration in a D. I. Diesel Engine," *SAE Paper* 952456.

Espey, C., Dec, J., Litzinger T. and Santavicca, D., 1997, "Planar Laser Rayleigh Scattering for Quantitative Vapor-Fuel Imaging in a Diesel Jet," *Combustion and Flame*, Vol. 109, pp. 65~86.

Felton, P., Bracco F. and Bardsley, M., 1993, "On the Quantitative Application of Exciplex Fluorescence to Engine Sprays," *SAE Paper* 930870.

Kim, T and Ghandhi, J. B. 2001, "Quantitative 2-D Fuel Vapor Concentration Measurements in an Evaporating Diesel Spray using the Exciplex Fluorescence Method," *SAE Paper* 2001-01-3495.

Kim, T., 2001, Quantitative 2-D Fuel Vapor Concentration Measurements in an Evaporating Diesel Spray using the Exciplex Fluorescence Method, Ph. D. diss., Department of Mechanical Engineering, University of Wisconsin, Madison,

Wisconsin.

Kosaka, H. and Kamimoto, T., 1993, "Quantitative Measurement of Fuel Vapor Concentration in an Unsteady Evaporating Spray via a 2-D Mie-scattering Imaging Technique," *SAE paper* 932653.

Melton, L., 1983, "Spectrally Separated Fluorescence Emissions for Diesel Fuel Droplets and Vapor," *Applied Optics*, Vol. 22, No. 14, pp. 2224~2226.

Naber, J. and Siebers, D., 1996, "Effects of Gas Density and Vaporization on Penetration and Dispersion of Diesel Sprays," *SAE Paper* 960034.

Oren, D., Wahiduzzaman, S. and Ferguson, C., 1984, "A Diesel Combustion Bomb : Proof of Concept," *SAE Paper* 841358.

Rabenstein, F., Egermann, J., Leipertz A. and D'Alfonso, N., 1998, "Vapor-Phase Structures of Diesel-Type Fuel Sprays : An Experimental Analysis," *SAE Paper* 982543.

Rotunno, A., Winter, M., Dobbs G., and Melton, L., 1990, "Direct Calibration Procedures for Exciplex-Based Vapor/Liquid Visualization of Fuel Sprays," *Combust. Sci. and Tech.*, Vol. 71, pp. 247~261.

Scheid, E., Pischinger, F., Knoche, K., Daams, H., Hassel E. and Ruter, U., 1986, "Spray Combustion Chamber with Optical Access, Ignition Zone Visualization and First Raman Measurements of Local Air-Fuel Ratio," *SAE Paper* 861121.

Senda J. and Kanda, T., 1997, "Quantitative Analysis of Fuel Vapor Concentration in Diesel Spray by Exciplex Fluorescence Method," *SAE paper* 970796.

Siebers, D., 1999, "Scaling Liquid-Phase Fuel Penetration in Diesel Sprays Based on Mixing-Limited Vaporization," *SAE Paper* 1999-01-0528.

Vargaftik, N. B., 1983, *Handbook of Physical Properties of Liquid and Gas*, Hemisphere, Washington.

Yaws, C. L., 1992, *Thermodynamic and Physical Property Data*, Gulf Publishing Company.

Yeh, C., Kamimoto, T., Kosaka H. and Kobori, S., 1994, "Quantitative Measurement of 2-D Fuel Vapor Concentration in a Transient Spray via Laser-Induced Fluorescence Technique," *SAE paper* 941953.

Zhao, H. and Ladommatos, N., 1998, "Optical Diagnostics for In-cylinder Mixture Formation Measurements in IC Engines," *Prog. Energy Combust. Sci.*, Vol. 24, pp. 297~336.